
Fourier Neural Operator-Based Models for Solving the Shallow Water Equations in Spherical Coordinates

Melissa Ulsøe Jessen (s194322)

Supervisor: DTU Compute
Co-supervisor: DTU Compute



Master Thesis
Mathematical Modelling and Computation

DTU Compute
Technical University of Denmark
February 2, 2025

Fourier Neural Operator-Based Models for Solving the Shallow Water Equations in Spherical Coordinates

Melissa Ulsøe Jessen (s194322)

October 17, 2024

Abstract

This master thesis focuses on the numerical and data-driven solutions for the Shallow Water Equations (SWE), which are fundamental in computational fluid dynamics. The project aims to solve the SWE using the Finite Volume Method (FVM) in 2D and spherical coordinates and subsequently exploit machine learning techniques, particularly the Fourier Neural Operator (FNO), to improve solution accuracy and efficiency. By the end of the project, the goal is to have a robust and efficient computational toolkit for solving the SWE, which will also be useful for simulating important geophysical processes like Kelvin and Rossby waves.

Notes

40 years ago Lax and Wendroff [116] proved mathematically that conservative numerical methods, if convergent, do converge to correct solutions of the equations. More recently, Hou and LeFloch [91] proved a complementary theorem which says that if a non-conservative method is used, then the wrong solution will be computed if this contains a shock wave.

Spurious oscillations are unavoidable if one uses linear methods of accuracy greater than one.

Gudonov's theorem: all (linear) schemes of accuracy greater than one will provide spurious oscillations. One must use non-linear methods, even when applied to linear problems.

A successful new class of shock-capturing numerical methods are the so-called high-resolution methods. High-resolution methods = Oscillation-free near shock waves, and retain second-order accuracy in smooth parts of the flow.

Gudonov methods are shock-capturing upwind methods. He later proposed a very fast exact Riemann solver and also approximate Riemann solvers.

a: the generalisation of Gudonov's first-order method to second-order accuracy by van Leer. b: the development of new approximate Riemann solvers by Roe and others.

TVD = Total Variation Diminishing.

More advanced, not presented in this book are UNO, ENO and WENO methods. Also the discontinuous Galerkin finite element method, combining FEM and Gudonov theory.

Trento course: - Day 2: SWE is a non-linear scalar equation/ conservation law

Contents

1	Introduction	1
1.1	Motivation	1
1.2	Literature	1
1.3	Thesis overview	1
2	Theory	2
2.1	Notation	2
2.2	The SWE with conservative variables	3
2.2.1	Conservation laws	3
2.2.2	Boundary conditions	4
2.2.3	Assumptions	5
2.2.4	Integration over depth	6
2.2.5	The SWE in vector form for 1D and 2D	8
2.2.6	The SWE in integral form	8
2.2.7	SWE in Spherical Coordinates	10
2.3	Finite Volume Method for the Shallow Water Equations	10
2.3.1	Finite Volume Methods for the 1D SWE	10
2.3.2	Finite Volume Method for the 2D SWE	12
2.4	The Riemann problem	12
2.4.1	Waves in the Riemann problem	13
2.4.2	Exact Riemann solver	14
2.5	Fourier Neural Operators and Neural Networks	14

3	Methodology	15
3.1	Approximate Riemann solvers	15
3.1.1	HLL solver	15
3.1.2	Roe solver	15
3.2	Implementation of the FVM in 1D	16
3.3	Godunov's Method	17
3.4	Data generation	17
4	Numerical results	19
4.1	The 1D Dam Break Problem	19
4.2	Toro test cases	20
	Test case 1	20
	Test case 2	21
	Test case 3	21
	Test case 4	22
	Test case 5	23
4.3	2D idealised Circular Dam Break Problem	23
5	Discussion	26
6	Further work	27
	Bibliography	28

Chapter 1

Introduction

This master thesis focuses on the numerical and data-driven solutions for the Shallow Water Equations (SWE), which are fundamental in computational fluid dynamics. The project aims to solve the SWE using the Finite Volume Method (FVM) in 2D and spherical coordinates and subsequently exploit machine learning techniques, particularly the Fourier Neural Operator (FNO), to improve solution accuracy and efficiency. By the end of the project, the goal is to have a robust and efficient computational toolkit for solving the SWE, which will also be useful for simulating important geophysical processes like Kelvin and Rossby waves.

The Shallow Water Equations (SWE) are a set of hyperbolic partial differential equations that describe the motion of a fluid in a shallow layer of water. In this project, we will derive the SWE in 1D, 2D and in spherical coordinates, to model the flow of water on the surface of the Earth. We will go through the Finite Volume Method (FVM) in 1D and 2D, which is a numerical method for solving partial differential equations by dividing the domain into small control volumes and integrating the equations over these volumes. The method is widely used in computational fluid dynamics to model the behavior of fluid flows. We will implement the FVM and use it to solve the SWE in 1D for two different dam break problems.

1.1 Motivation

1.2 Literature

1.3 Thesis overview

Chapter 2

Theory

In this chapter we will derive the shallow water equations (SWE) in conservative form, and present the equations in vector form and in integral form for 1D and 2D.

2.1 Notation

Before deriving the shallow water equations (SWE), we will introduce the notation that will be used throughout this report. In both the 1D case and the 2D case of SWE, we use cartesian coordinates (x, y, z) with time denoted by t . Given that linear algebra is a fundamental tool used in this report, we first establish the relevant notation. Lowercase bold letters represent vectors, while uppercase bold letters represent matrices. For instance, \mathbf{a} is a vector of size $r \times 1, r \in \mathbb{R}$, and \mathbf{A} is a matrix of size $m \times n, m, n \in \mathbb{R}$. The identity matrix, denoted by \mathbf{I} , is a square matrix with ones along the diagonal and zeros elsewhere. For example, the 3×3 identity matrix is given by:

$$\mathbf{I} = \begin{bmatrix} 1 & 0 & 0 \\ 0 & 1 & 0 \\ 0 & 0 & 1 \end{bmatrix}.$$

We use the following notation for partial derivatives:

$$f_x = \frac{\partial f}{\partial x}, \quad f_y = \frac{\partial f}{\partial y}, \quad f_z = \frac{\partial f}{\partial z}. \quad (2.1.1)$$

The gradient operator, denoted by ∇ , gives the gradient of a scalar function $f(x, y, z)$ as a vector:

$$\nabla f = \begin{bmatrix} \frac{\partial f}{\partial x} & \frac{\partial f}{\partial y} & \frac{\partial f}{\partial z} \end{bmatrix}.$$

Given two vectors $\mathbf{a} = [a_1 \quad a_2 \quad a_3]^\top$ and $\mathbf{b} = [b_1 \quad b_2 \quad b_3]^\top$, the dot product of \mathbf{a} and \mathbf{b} is given by:

$$\mathbf{a} \cdot \mathbf{b} = a_1 b_1 + a_2 b_2 + a_3 b_3.$$

The dot product can also be written as a matrix product:

$$\mathbf{a} \cdot \mathbf{b} = \mathbf{a}^\top \mathbf{b}.$$

The divergence operator, represented as $\nabla \cdot$, gives the divergence of a vector \mathbf{a} as:

$$\nabla \cdot \mathbf{a} = \frac{\partial a_1}{\partial x} + \frac{\partial a_2}{\partial y} + \frac{\partial a_3}{\partial z} = a_{1x} + a_{2y} + a_{3z},$$

using the notation for partial derivatives introduced in (2.1.1). The tensor product of two vectors \mathbf{a} and \mathbf{b} , denoted as $\mathbf{a} \otimes \mathbf{b}$, is a matrix where each element is the product of the elements of \mathbf{a} and \mathbf{b} , i.e.,

$$\mathbf{a} \otimes \mathbf{b} = \begin{bmatrix} a_1 b_1 & a_1 b_2 & a_1 b_3 \\ a_2 b_1 & a_2 b_2 & a_2 b_3 \\ a_3 b_1 & a_3 b_2 & a_3 b_3 \end{bmatrix}.$$

Establishing this relevant notation, we can now derive the shallow water equations in 1D and 2D.

2.2 The SWE with conservative variables

In this section we will derive the shallow water equations (SWE) in conservative form. The derivation follows four steps: First we consider the conservation laws for mass and momentum, and then we consider the boundary conditions for a free surface problem. Afterwards we make some necessary assumptions and finally we use the boundary conditions to integrate the conservation laws over depth. The derivation follows the methods outlined in [1] and [2].

2.2.1 Conservation laws

The SWE are derived from the conservation laws for mass and momentum, which are fundamental in fluid dynamics. The conservation laws for mass and momentum can be expressed generally as follows (see eq. (2.1) and (2.2) in [1]):

$$\rho_t + \nabla \cdot (\rho \mathbf{v}) = 0, \quad (2.2.1)$$

$$(\rho \mathbf{v})_t + \nabla \cdot (\rho \mathbf{v} \otimes \mathbf{v} + p \mathbf{I} - \mathbf{T}) = \rho \mathbf{g}, \quad (2.2.2)$$

where ρ is the fluid density, $\mathbf{v} = [u \ v \ w]^\top$ is the fluid velocity in the x, y and z -direction respectively; p is the pressure, \mathbf{I} is the identity matrix, and the vector $\mathbf{g} = [g_1 \ g_2 \ g_3]^\top$ represents body forces including gravity. In these equations, the density ρ and the pressure p are dependent of x, y, z and t , but later we will introduce some assumptions that simplify the equations. The matrix \mathbf{T} is the viscous stress tensor, given by

$$\mathbf{T} = \begin{bmatrix} \tau_{xx} & \tau_{xy} & \tau_{xz} \\ \tau_{yx} & \tau_{yy} & \tau_{yz} \\ \tau_{zx} & \tau_{zy} & \tau_{zz} \end{bmatrix},$$

which accounts for the viscous forces in the fluid. However, in this project the viscous stress tensor \mathbf{T} is neglected, since we assume the function $\tau(x, y, z)$ is constant. The matrix $\mathbf{v} \otimes \mathbf{v}$ represents the tensor product of the velocity vector \mathbf{v} with itself, i.e.,

$$\mathbf{v} \otimes \mathbf{v} = \begin{bmatrix} u^2 & uv & uw \\ vu & v^2 & vw \\ wu & wv & w^2 \end{bmatrix}.$$

Note that $\mathbf{v} \otimes \mathbf{v} = \mathbf{v} \mathbf{v}^\top$. Putting this together, we can rewrite the momentum equation (2.2.2) as

$$(\rho \mathbf{v})_t + \nabla \cdot (\rho \mathbf{v} \mathbf{v}^\top + p \mathbf{I}) - \rho \mathbf{g} = 0. \quad (2.2.3)$$

In this project we consider incompressible fluids, meaning that the fluid density ρ is independent of the pressure p . We also assume that the fluid density only depends on temperature and salinity, and thus is independent of t, x, y and z . Additionally, we assume ρ is nonzero. Using these assumptions and the product rule for differentiation, we can simplify the mass conservation equation (2.2.1) to

$$\rho_t + \rho(u_x + v_y + w_z) + u\rho_x + v\rho_y + w\rho_z = 0,$$

implying that

$$u_x + v_y + w_z = 0. \quad (2.2.4)$$

Applying the divergence operator $\nabla \cdot$, the momentum conservation equation (2.2.3) can be written out as:

$$\rho_t \mathbf{v} + \rho \mathbf{v}_t + \rho \begin{bmatrix} (u^2 + p)_x + (uv)_y + (uw)_z \\ (vu)_x + (v^2 + p)_y + (vw)_z \\ (wu)_x + (wv)_y + (w^2 + p)_z \end{bmatrix} - \rho \mathbf{g} = 0. \quad (2.2.5)$$

We neglect all body forces in \mathbf{g} , expect the gravitational force in the z -direction, i.e., $\mathbf{g} = [0 \ 0 \ -g]$, where g is the gravity acceleration. Hence, by using the product rule in (2.2.5) we obtain

$$\rho \begin{bmatrix} u_t \\ v_t \\ w_t \end{bmatrix} + \rho \begin{bmatrix} p_x + uu_x + vu_y + wu_z + u(u_x + v_y + w_z) \\ p_y + uv_x + vv_y + wv_z + v(u_x + v_y + w_z) \\ p_z + uw_x + vw_y + ww_z + w(u_x + v_y + w_z) \end{bmatrix} - \rho \begin{bmatrix} 0 \\ 0 \\ -g \end{bmatrix} = 0. \quad (2.2.6)$$

We apply (2.2.4) to (2.2.6) to remove some terms, we move the pressure terms to the right hand side, and we divide by ρ . Putting it all together, the mass equation (2.2.1) and the momentum equation (2.2.3), split in x, y and z -directions, simplify to

$$\left. \begin{aligned} u_x + v_y + w_z &= 0, \\ u_t + uu_x + vu_y + wu_z &= -\frac{1}{\rho} p_x, \\ v_t + uv_x + vv_y + wv_z &= -\frac{1}{\rho} p_y, \\ w_t + uw_x + vw_y + ww_z &= -\frac{1}{\rho} p_z - g. \end{aligned} \right\} \quad (2.2.7)$$

2.2.2 Boundary conditions

In this project, we consider the flow of water with a free surface, meaning that the surface is not fixed and can move or change over time. To solve the SWE, it is essential to impose boundary conditions at both the bottom of the water column and the free surface. We assume the bottom boundary is defined by a function

$$z = b(x, y),$$

meaning that the bottom is dependent on x and y , but not on the time t . The free surface is defined by

$$z = s(x, y, t) \equiv b(x, y) + h(x, y, t),$$

where $h(x, y, t)$ is the water depth at time t . The following illustration helps to visualize the setup:

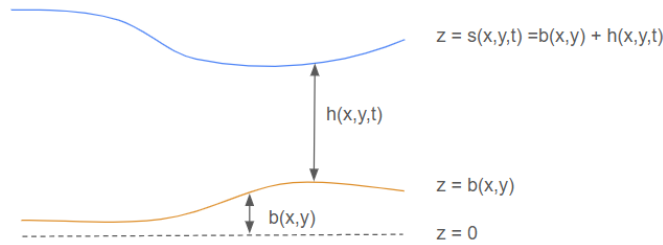


Figure 2.1: Illustration of a water column with a free surface.

We impose boundary conditions at the bottom and at the free surface, addressing both kinematic and dynamical conditions. To describe the boundaries mathematically, we introduce a boundary function $\psi(x, y, z, t)$ that is zero on a boundary:

$$\psi(x, y, z, t) = 0.$$

For the free surface, this boundary is given by

$$\psi(x, y, z, t) \equiv z - s(x, y, t) = 0, \quad (2.2.8)$$

and for the bottom, it is described by

$$\psi(x, y, z, t) \equiv z - b(x, y) = 0. \quad (2.2.9)$$

In the kinematic condition, we assume that fluid particles on the boundary remain on the boundary over time. Mathematically this is expressed as

$$\frac{d}{dt}\psi(x, y, z, t) = 0.$$

Recall, that $\frac{\partial \psi}{\partial t}$ is the partial derivative of ψ with respect to t , while the total derivative $\frac{d\psi}{dt}$ accounts for both the direct change of ψ with respect to t and the changes due to the movement of the fluid in the x, y and z directions. Hence, the total derivative of ψ wrt. t is given by

$$\frac{d\psi}{dt} = \frac{\partial \psi}{\partial t} + \frac{dx}{dt} \frac{\partial \psi}{\partial x} + \frac{dy}{dt} \frac{\partial \psi}{\partial y} + \frac{dz}{dt} \frac{\partial \psi}{\partial z}.$$

We see that $\frac{dx}{dt}$ denotes the velocity in the x -direction, i.e., u , and correspondingly $\frac{dy}{dt}$ and $\frac{dz}{dt}$ denotes v and w respectively. Thus, the kinematic condition is given by

$$\frac{d}{dt}\psi(x, y, z, t) = \psi_t + u\psi_x + v\psi_y + w\psi_z = 0. \quad (2.2.10)$$

Applying this to the free surface by substituting (2.2.8) into the kinematic condition (2.2.10) yields

$$(s_t + us_x + vs_y - w)|_{z=s} = 0. \quad (2.2.11)$$

Similarly, for the bottom, substituting (2.2.9) into the kinematic condition (2.2.10) gives

$$(ub_x + vb_y - w)|_{z=b} = 0. \quad (2.2.12)$$

The dynamical condition is related to the pressure distribution at the free surface. We assume that the pressure at the free surface is equal to the pressure in the air above the surface, that is, the atmospheric pressure. Since absolute pressure levels are irrelevant (we are primarily concerned with pressure differences), we set the pressure at the free surface to zero. This leads to the following expression for the pressure at the free surface:

$$p(x, y, z, t)|_{z=s(x, y, t)} = 0. \quad (2.2.13)$$

This condition, known as the dynamical condition, relates to the forces acting on the boundaries of the fluid.

2.2.3 Assumptions

To derive the SWE it is necessary to make some assumptions. The shallow water equations are an approximation to the full free-surface problem and result from the assumption that the vertical component of the acceleration

is negligible. Therefore, we begin by assuming that the vertical acceleration, represented by the total derivative of the vertical velocity component w with respect to time, is negligible. This assumption leads to the condition

$$\frac{dw}{dt} = w_t + uw_x + vw_y + ww_z = 0.$$

Applying $\frac{dw}{dt} = 0$ in the z -momentum conservation equation (2.2.7) simplifies it to

$$p_z = -\rho g.$$

By using properties of an integral, together with (2.2.13) we get

$$\int_{b(x,y)}^z -\rho g \, dz + \int_z^{s(x,y,t)} -\rho g \, dz = \int_{b(x,y)}^{s(x,y,t)} -\rho g \, dz = p|_{z=s(x,y,t)} - p|_{z=b(x,y)} = 0.$$

This implies that the pressure distribution follows

$$p = \int_{b(x,y)}^z -\rho g \, dz = \int_z^{s(x,y,t)} \rho g \, dz = \rho g(s - z), \quad (2.2.14)$$

where s is the surface height. Differentiating (2.2.14) with respect to x and y yields

$$p_x = \rho g s_x, \quad p_y = \rho g s_y.$$

Substituting these expressions into the x - and y -momentum conservation equations (2.2.7) leads to

$$u_t + uu_x + vu_y + wu_z = -gs_x, \quad (2.2.15)$$

and

$$v_t + uv_x + vv_y + wv_z = -gs_y. \quad (2.2.16)$$

These are the simplified momentum equations for the shallow water equations. We realize that both p_x and p_y are independent of z , implying that $\frac{du}{dt}$ and $\frac{dv}{dt}$ are also independent of z . Hence $u_z = v_z = 0$, implying that (2.2.15) and (2.2.16) can be simplified to

$$u_t + uu_x + vu_y = -gs_x, \quad (2.2.17)$$

and

$$v_t + uv_x + vv_y = -gs_y. \quad (2.2.18)$$

2.2.4 Integration over depth

The next step in deriving the SWE is to integrate the conservation equations over the vertical direction z . We integrate the mass conservation equation (2.2.4) and the x - and y -momentum conservation equations in (2.2.7), from the bottom, $z = b(x, y)$ to the free surface, $z = s(x, y, t)$. Starting with the mass conservation equation (2.2.4), we have

$$\int_b^s (u_x + v_y + w_z) \, dz = 0,$$

implying that, using linearity of the integral:

$$\int_b^s u_x \, dz + \int_b^s v_y \, dz + w|_{z=s} - w|_{z=b} = 0. \quad (2.2.19)$$

We will use Leibniz's integral rule [3], which is stated as follows:

$$\frac{d}{dx} \int_{a(x)}^{b(x)} f(x, t) dt = \int_{a(x)}^{b(x)} \frac{\partial}{\partial x} f(x, t) dt + f(x, b(x)) \frac{d}{dx} b(x) - f(x, a(x)) \frac{d}{dx} a(x), \quad (2.2.20)$$

to integrate the first two terms in (2.2.19), which yields

$$\left. \begin{aligned} \int_b^s u_x dz &= \frac{d}{dx} \int_b^s u dz - u|_{z=s} \frac{ds}{dx} + u|_{z=b} \frac{db}{dx}, \\ \int_b^s v_y dz &= \frac{d}{dy} \int_b^s v dz - v|_{z=s} \frac{ds}{dy} + v|_{z=b} \frac{db}{dy}. \end{aligned} \right\} \quad (2.2.21)$$

Note that since a change in x does not affect the y -component of the bottom or surface, we have that $\frac{ds}{dx} = s_x$ and $\frac{db}{dx} = b_x$, and correspondingly for s_y and b_y . Likewise we can substitute $\frac{d}{dx}$ with $\frac{\partial}{\partial x}$ in the integrals, since the integrals are with respect to z , and u and v are independent of z . Inserting these results in (2.2.21) gives

$$\left. \begin{aligned} \int_b^s u_x dz &= \frac{\partial}{\partial x} \int_b^s u dz - u|_{z=s} s_x + u|_{z=b} b_x, \\ \int_b^s v_y dz &= \frac{\partial}{\partial y} \int_b^s v dz - v|_{z=s} s_y + v|_{z=b} b_y. \end{aligned} \right\} \quad (2.2.22)$$

We can now insert the integrals (2.2.22) into the integrated mass conservation equation (2.2.19) to get

$$\frac{\partial}{\partial x} \int_b^s u dz - u|_{z=s} s_x + u|_{z=b} b_x + \frac{\partial}{\partial y} \int_b^s v dz - v|_{z=s} s_y + v|_{z=b} b_y + w|_{z=s} - w|_{z=b} = 0. \quad (2.2.23)$$

To simplify this equation further, we consider the boundary conditions. From (2.2.12) we have

$$w|_{z=b} = (ub_x + vb_y)|_{z=b}, \quad (2.2.24)$$

and from (2.2.11) we have

$$w|_{z=s} = (s_t + us_x + vs_y)|_{z=s}. \quad (2.2.25)$$

We note that $s = b + h$ and hence $s_t = h_t$, as the bottom is fixed. Recall that u and v are independent of z , and the water depth is $h = s - b$, meaning we have

$$\int_b^s u dz = u(s - b) = hu, \quad \int_b^s v dz = v(s - b) = hv.$$

Putting it all together the equation (2.2.23) simplifies to

$$h_t + (hu)_x + (hv)_y = 0, \quad (2.2.26)$$

which is also the first equation in the SWE in conservative form. When integrating the momentum equations (2.2.17) and (2.2.18) over the vertical direction, we see that since the equations are independent of z , the resulting equations are simply

$$h(u_t + uu_x + vu_y + gs_x) = 0, \quad (2.2.27)$$

$$h(v_t + uv_x + vv_y + gs_y) = 0. \quad (2.2.28)$$

We multiply (2.2.26) with u and v respectively, and add the resulting two equations to (2.2.27) and (2.2.28) correspondingly. Recall that $s = h + b$. By using the product rule for differentiation and collecting terms, we obtain the momentum equations in conservative form:

$$(hu)_t + (hu^2 + \frac{1}{2}gh^2)_x + (huv)_y = -ghb_x, \quad (2.2.29)$$

and

$$(hv)_t + (huv)_x + (hv^2 + \frac{1}{2}gh^2)_y = -ghb_y. \quad (2.2.30)$$

The three partial differential equations in (2.2.26), (2.2.29) and (2.2.30) are the shallow water equations in conservative form.

2.2.5 The SWE in vector form for 1D and 2D

The SWE can also be written in differential conservation law form as a vector equation

$$\mathbf{U}_t + \mathbf{F}(\mathbf{U})_x + \mathbf{G}(\mathbf{U})_y = \mathbf{S}(\mathbf{U}), \quad (2.2.31)$$

where

$$\mathbf{U} = \begin{bmatrix} h \\ hu \\ hv \end{bmatrix}, \quad \mathbf{F}(\mathbf{U}) = \begin{bmatrix} hu \\ hu^2 + \frac{1}{2}gh^2 \\ huv \end{bmatrix}, \quad \mathbf{G}(\mathbf{U}) = \begin{bmatrix} hv \\ huv \\ hv^2 + \frac{1}{2}gh^2 \end{bmatrix} \quad \text{and} \quad \mathbf{S}(\mathbf{U}) = \begin{bmatrix} s_1 \\ s_2 \\ s_3 \end{bmatrix} = \begin{bmatrix} 0 \\ -ghb_x \\ -ghb_y \end{bmatrix}.$$

We call \mathbf{U} the vector of conserved variables, $\mathbf{F}(\mathbf{U})$ and $\mathbf{G}(\mathbf{U})$ the flux vectors in the x and y direction, and $\mathbf{S}(\mathbf{U})$ the source term vector.

Homogeneous 1D case:

In this project, we will begin by considering the homogeneous one-dimensional case of the shallow water equations. In the homogeneous case we assume that $\mathbf{S}(\mathbf{U}) = 0$. The vector form of the SWE in 1D is then given by

$$\mathbf{U}_t + \mathbf{F}(\mathbf{U})_x = 0,$$

where

$$\mathbf{U} = \begin{bmatrix} h \\ hu \end{bmatrix}, \quad \text{and} \quad \mathbf{F}(\mathbf{U}) = \begin{bmatrix} hu \\ hu^2 + \frac{1}{2}gh^2 \end{bmatrix}.$$

In the 1D case, we only consider flow in the x -direction.

Inhomogeneous 1D case:

The inhomogeneous one-dimensional case of the shallow water equations in vector form is given by

$$\mathbf{U}_t + \mathbf{F}(\mathbf{U})_x = \mathbf{S}(\mathbf{U}), \quad (2.2.32)$$

where

$$\mathbf{U} = \begin{bmatrix} h \\ hu \end{bmatrix}, \quad \mathbf{F}(\mathbf{U}) = \begin{bmatrix} hu \\ hu^2 + \frac{1}{2}gh^2 \end{bmatrix} \quad \text{and} \quad \mathbf{S}(\mathbf{U}) = \begin{bmatrix} 0 \\ -ghb_x \end{bmatrix}. \quad (2.2.33)$$

If $\mathbf{S}(\mathbf{U}) = 0$, the equation (2.2.32) is called a conservation law, and otherwise it is called a balance law.

2.2.6 The SWE in integral form

It is often more convenient to work with the integral form of the SWE, since the integral form of equations of the form (2.2.32) and (2.2.33) allows discontinuous solutions. The integral form is obtained by integrating the vector form (2.2.32) over a control volume V in the $x - t$ plane

$$V = [x_L, x_R] \times [t_1, t_2].$$

The control volume is illustrated in Figure 2.2.

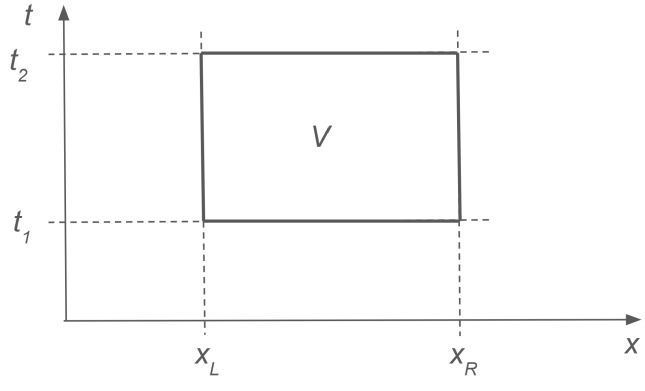


Figure 2.2: Illustration of a control volume V in the $x-t$ plane. Illustration modified from [4].

First we integrate the vector form of the SWE (2.2.32) over x from x_L to x_R to obtain

$$\int_{x_L}^{x_R} \mathbf{U}_t \, dx + \int_{x_L}^{x_R} \mathbf{F}(\mathbf{U})_x \, dx = \int_{x_L}^{x_R} \mathbf{S}(\mathbf{U}) \, dx. \quad (2.2.34)$$

Using the fundamental theorem of calculus, we get that

$$\int_{x_L}^{x_R} \mathbf{F}(\mathbf{U}) \, dx = \mathbf{F}(\mathbf{U}(x_R, t)) - \mathbf{F}(\mathbf{U}(x_L, t)),$$

which we insert in (2.2.34):

$$\int_{x_L}^{x_R} \mathbf{U}_t \, dx = \mathbf{F}(\mathbf{U}(x_L, t)) - \mathbf{F}(\mathbf{U}(x_R, t)) + \int_{x_L}^{x_R} \mathbf{S}(\mathbf{U}) \, dx. \quad (2.2.35)$$

Then we integrate (2.2.35) over time from t_1 to t_2 to get

$$\int_{t_1}^{t_2} \int_{x_L}^{x_R} \mathbf{U}_t \, dx dt = \int_{t_1}^{t_2} \mathbf{F}(\mathbf{U}(x_L, t)) \, dt - \int_{t_1}^{t_2} \mathbf{F}(\mathbf{U}(x_R, t)) \, dt + \int_{t_1}^{t_2} \int_{x_L}^{x_R} \mathbf{S}(\mathbf{U}) \, dx dt.$$

Rewriting the left hand side using the fundamental theorem of calculus, we get

$$\int_{x_L}^{x_R} \mathbf{U}(x, t_2) \, dx = \int_{x_L}^{x_R} \mathbf{U}(x, t_1) \, dx + \int_{t_1}^{t_2} \mathbf{F}(\mathbf{U}(x_L, t)) \, dt - \int_{t_1}^{t_2} \mathbf{F}(\mathbf{U}(x_R, t)) \, dt + \int_{t_1}^{t_2} \int_{x_L}^{x_R} \mathbf{S}(\mathbf{U}) \, dx dt, \quad (2.2.36)$$

which is the integral form of the conservation laws for the SWE in 1D. An alternative integral form of (2.2.32) is stated in [4]:

$$\frac{d}{dt} \int_{x_L}^{x_R} \mathbf{U}(x, t) \, dx = \mathbf{F}(\mathbf{U}(x_L, t)) - \mathbf{F}(\mathbf{U}(x_R, t)) + \int_{x_L}^{x_R} \mathbf{S}(\mathbf{U})(x, t) \, dx. \quad (2.2.37)$$

From (2.2.37) we get that the integral form of the homogeneous SWE in 1D is given by

$$\frac{d}{dt} \int_{x_L}^{x_R} \mathbf{U}(x, t) \, dx = \mathbf{F}(\mathbf{U}(x_L, t)) - \mathbf{F}(\mathbf{U}(x_R, t)), \quad (2.2.38)$$

meaning that the rate of change of the integral over a domain is equal to the flux through the boundaries of the domain.

2.2.7 SWE in Spherical Coordinates

TBD.

2.3 Finite Volume Method for the Shallow Water Equations

In this section we will describe the Finite Volume Method (FVM) for solving nonlinear systems of balance laws, such as the shallow water equations (SWE). That is, we consider the FVM for nonlinear hyperbolic conservation laws, such as the shallow water equations. The nonlinear case is obviously more challenging than the linear case, as stability and convergence theory are more difficult. We are interested in discontinuous solutions, which can capture shock waves and other discontinuities in the solution. The method described is based on the book by LeVeque [5].

In finite volume methods, we discretize the domain into cells or control volumes. Then we solve the local Riemann problem at the cell interface to obtain the fluxes. Using the computed fluxes, we update the solution in each cell. This way, the FVM allows for discontinuous solutions, as we solve the Riemann problem at the cell interfaces. Therefore it is well suited for hyperbolic conservation laws, such as the shallow water equations.

2.3.1 Finite Volume Methods for the 1D SWE

We begin by considering finite volume methods for the SWE in one space dimension. In the FVM, we discretize the domain into finite control volumes or cells:

$$V_i = [x_{i-1/2}, x_{i+1/2}] \times [t_n, t_{n+1}],$$

where $\Delta x = x_{i+1/2} - x_{i-1/2}$ is the length of the cell and $\Delta t = t_{n+1} - t_n$ is the time step. The cell V_i is illustrated in Figure 2.3.

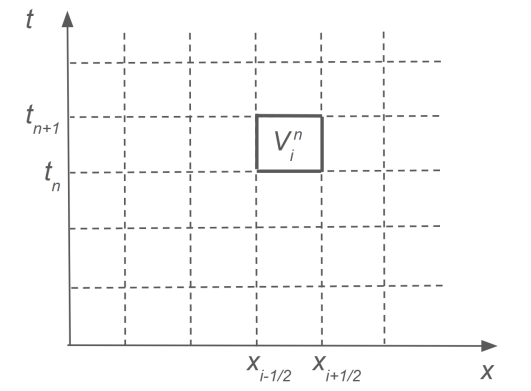


Figure 2.3: Illustration of the control volume V_i^n in the $x-t$ plane.

For now, we will assume a uniform grid for simplicity. The Finite Volume Formula is derived from the integral

form (2.2.36). By dividing this by the cell length Δx , we express it in terms of the newly defined cells:

$$\begin{aligned} \frac{1}{\Delta x} \int_{x_{i-1/2}}^{x_{i+1/2}} \mathbf{U}(x, t_{n+1}) dx &= \frac{1}{\Delta x} \int_{x_{i-1/2}}^{x_{i+1/2}} \mathbf{U}(x, t_n) dx \\ &\quad - \frac{\Delta t}{\Delta x} \left[\frac{1}{\Delta t} \int_{t_n}^{t_{n+1}} \mathbf{F}(\mathbf{U}(x_{i+1/2}, t)) dt - \frac{1}{\Delta t} \int_{t_n}^{t_{n+1}} \mathbf{F}(\mathbf{U}(x_{i-1/2}, t)) dt \right] \\ &\quad + \frac{\Delta t}{\Delta x \Delta t} \int_{x_{i-1/2}}^{x_{i+1/2}} \int_{t_n}^{t_{n+1}} \mathbf{S}(\mathbf{U})(x, t) dx dt. \end{aligned}$$

For a finite volume V_i^n , averaging the terms over the volume yields the explicit conservative form

$$\mathbf{U}_i^{n+1} = \mathbf{U}_i^n - \frac{\Delta t}{\Delta x} (\mathbf{F}_{i+1/2}^n - \mathbf{F}_{i-1/2}^n) + \Delta t \mathbf{S}_i. \quad (2.3.1)$$

Here, \mathbf{U}_i^n is the average value over the i -th cell at time t_n :

$$\mathbf{U}_i^n = \frac{1}{\Delta x} \int_{x_{i-1/2}}^{x_{i+1/2}} \mathbf{U}(x, t_n) dx, \quad (2.3.2)$$

also known as the cell average. The flux $\mathbf{F}_{i-1/2}^n$ is the average flux across the line $x = x_{i-1/2}$ at time t_n :

$$\mathbf{F}_{i-1/2}^n = \frac{1}{\Delta t} \int_{t_n}^{t_{n+1}} \mathbf{F}(\mathbf{U}(x_{i-1/2}, t)) dt,$$

while the source term \mathbf{S}_i is the average source term over the i -th cell at time t_n :

$$\mathbf{S}_i = \frac{1}{\Delta t \Delta x} \int_{t_n}^{t_{n+1}} \int_{x_{i-1/2}}^{x_{i+1/2}} \mathbf{S}(x, t) dx dt.$$

The values are illustrated in Figure 2.4.

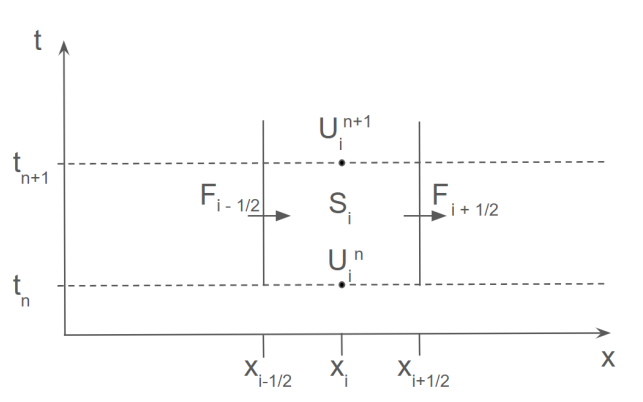


Figure 2.4: Illustration of the grid for the 1D SWE.

The FVM involves discretizing the domain into finite control volumes or cells. At each cell interface, the local Riemann problem is solved to compute the fluxes, which are then used to update the solution in each cell. This approach allows for discontinuous solutions, as the Riemann problem is solved at the cell interfaces. Thus, the FVM is particularly well suited for hyperbolic conservation laws, such as the shallow water equations.

In the context of the 1D Shallow Water Equations (SWE), the FVM is applied by dividing the spatial domain into a set of intervals or grid cells. Figure 2.5 illustrates the grid structure used,

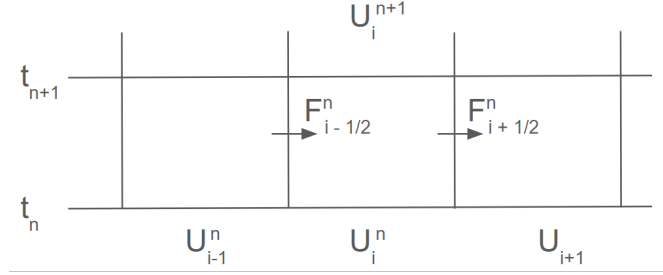


Figure 2.5: Illustration of the grid for the 1D SWE.

This method, represented by the formula (2.3.1), is referred to as a finite volume scheme, since it is based on the integral conservation over finite volumes.

Finite volume methods are closely related to finite difference methods, but they differ as they are based on the integral form of the conservation laws. Where finite difference methods tend to break down near discontinuities in the solution, finite volume methods are more suited, since they are based on the integral form of the conservation laws. The key distinction between the FVM and the Finite Difference Method (FDM) lies in their formulation: while the FVM is based on the integral conservation over finite volumes, the FDM is based on the differential conservation over finite differences.

The central idea of the FVM is to define the numerical flux $\mathbf{F}_{i+1/2}^n$, at the cell interface, as a function of the cell averages \mathbf{U}_i^n and \mathbf{U}_{i+1}^n , since the solution is known only in terms of these cell averages. Consequently, the FVM does not provide pointwise values of the solution, i.e., $\mathbf{U}(x, t)$, but instead gives cell-averaged values, \mathbf{U}_i^n , over the control volume. One of the main challenges in the FVM is to determine appropriate numerical flux functions that, based on the available cell averages, can reasonably approximate the fluxes at the cell interfaces.

2.3.2 Finite Volume Method for the 2D SWE

Follows the methods outlined in [6]. Consider a time-dependent two dimensional system of conservation laws

$$\mathbf{U}_t + \mathbf{F}(\mathbf{U})_x + \mathbf{G}(\mathbf{U})_y = 0. \quad (2.3.3)$$

A numerical explicit finite volume scheme to solve (2.3.3) is given by

$$\mathbf{U}_{i,j}^{n+1} = \mathbf{U}_{i,j}^n + \frac{\Delta t}{\Delta x} (\mathbf{F}_{i-1/2,j} - \mathbf{F}_{i+1/2,j}) + \frac{\Delta t}{\Delta y} (\mathbf{G}_{i,j-1/2} - \mathbf{G}_{i,j+1/2}). \quad (2.3.4)$$

This is the unsplit finite volume method, meaning that, in a single step, the cell average $\mathbf{U}_{i,j}^n$ is updated using the fluxes from all intercell boundaries.

2.4 The Riemann problem

We will now define the Riemann problem, since it plays a crucial role in the finite volume method. In the Riemann problem we distinguish between what we call a wet bed and a dry bed. A wet bed is the case where the water depth is positive everywhere, whereas a dry bed is the case where the water depth is zero in some cells. The special Riemann problem where parts of the bed are dry is dealing with the so-called dry fronts or wet/dry fronts, which are challenging to handle numerically. We will leave these cases for now, and only consider the wet bed problems.

The Riemann problem for the shallow water equations is defined as the initial-value problem (IVP) [4]:

$$\begin{aligned} \text{PDEs: } \mathbf{U}_t + \mathbf{F}(\mathbf{U})_x &= 0, \\ \text{ICs: } \mathbf{U}(x, 0) &= \begin{cases} \mathbf{U}_L, & \text{if } x < 0, \\ \mathbf{U}_R, & \text{if } x > 0. \end{cases} \end{aligned} \quad (2.4.1)$$

Here, the vectors \mathbf{U} and $\mathbf{F}(\mathbf{U})$ in (2.4.1) are given By

$$\mathbf{U} = \begin{bmatrix} h \\ hu \\ hv \end{bmatrix}, \quad \mathbf{F}(\mathbf{U}) = \begin{bmatrix} hu \\ hu^2 + \frac{1}{2}gh^2 \\ hvu \end{bmatrix}, \quad (2.4.2)$$

and the initial conditions \mathbf{U}_L and \mathbf{U}_R are

$$\mathbf{U}_L = \begin{bmatrix} h_L \\ h_L u_L \\ h_L v_L \end{bmatrix}, \quad \mathbf{U}_R = \begin{bmatrix} h_R \\ h_R u_R \\ h_R v_R \end{bmatrix},$$

which represents the conditions at time $t = 0$ in the left and right states of $x = 0$, respectively. The function \mathbf{U} is piecewise constant, with a discontinuity at $x = 0$. The Riemann problem is a generalisation of the so-called dam-break problem. The difference is that in the Riemann problem the particle velocity components, u_L, u_R, v_L and v_R , are allowed to be distinct from zero, whereas in the dam-break problem, they must be zero.

The Riemann problem can be solved both exactly and approximately. There are several approximate Riemann solvers, such as the HLL and Roe solvers, which are based on the approximate solution of the Riemann problem. We will consider some of these solvers later in the thesis.

2.4.1 Waves in the Riemann problem

To get a better understanding of the flow in shallow water, we provide some very short background information about waves. In particular the wave structure in the solution of the Riemann problem (2.4.1).

What is a rarefaction and a shock wave?

In the solution of the Riemann problem (2.4.1) there are four possible wave patterns outcomes, which are combinations of shock waves and rarefaction waves. In each case there are three waves, the left and right waves correspond to the one-dimensional SWE, and the middle wave arises from the y -momentum equation in (2.4.1) and is always a shear wave. The left and right waves are either shock waves or rarefaction waves. The four possible wave patterns are illustrated in Figure XX and are as follows:

1. Left rarefaction, right shock
2. Left shock, right rarefaction
3. Both left and right rarefaction
4. Both left and right shock

Hence the structure of the solution in general is shown in the figure below. From the figure we see that the solution consists of three waves, a left wave, a middle wave and a right wave, which together separate four regions, described by the vector

$$\mathbf{W} = \begin{bmatrix} h \\ hu \\ hv \end{bmatrix}.$$

The four regions are describes by \mathbf{W}_L (left data), \mathbf{W}_R (right data), \mathbf{W}_{*L} and \mathbf{W}_{*R} , which both denote star region data. We are interested in the star region data, since these are the unknowns. We know that the left and right waves are always either a shock wave or a rarefaction wave, and the middle wave is always a shear wave. Based on the given initial conditions, we must determine the types of waves. Second, it is known that across the left and right waves, both h and u change but v remains constant. Whereas across the middle wave, v changes but h and u remain constant. Thus the water depth and particle velocity are constant in the star region and are denoted by h_* and u_* , respectively.

2.4.2 Exact Riemann solver

The exact Riemann solver presented in this section is very efficient and leads to Gudonov methods, that are only slightly more expensive than those based on approximate Riemann solvers [1]. Important to find the exact solution to the Riemann problem in the early stage of development, before moving on to more complex applications.

In the solution of the Riemann problem (2.4.1), there are four possible wave patterns outcomes, which are combinations of shock waves and rarefaction waves. In each case there are three waves, the left and right waves correspond to the one-dimensional SWE, and the middle wave arises from the y -momentum equation in (2.4.1). The left and right waves are either shock waves or rarefaction waves, and the middle wave is always a shear wave.

But for now, we will consider the case where the solution consists of a single non-trivial wave and all other waves are assumed to have zero strength. This is enough to solve the Riemann problem as it is always possible to solve the Riemann problem by considering one wave at a time.

We denote the constant values of the water depth and particle velocity in the star region by h_* and u_* , respectively.

2.5 Fourier Neural Operators and Neural Networks

TBD.

Chapter 3

Methodology

In this chapter..

3.1 Approximate Riemann solvers

We will study two approximate Riemann solvers to solve the Riemann problem (2.4.1), that is, the HLL and Roe.

3.1.1 HLL solver

The HLL (Harten, Lax and van Leer) approach assumes a two-wave structure of the Riemann problem, see Figure. The solver is based on the data $\mathbf{U}_L \equiv \mathbf{U}_i^n$, $\mathbf{U}_R \equiv \mathbf{U}_{i+1}^n$ and fluxes $\mathbf{F}_L \equiv \mathbf{F}(\mathbf{U}_L)$, $\mathbf{F}_R \equiv \mathbf{F}(\mathbf{U}_R)$.

The HLL flux is given by

$$\mathbf{F}_{1+\frac{1}{2}} = \begin{cases} \mathbf{F}_L & \text{if } S_L \geq 0, \\ \mathbf{F}^{hll} \equiv \frac{S_R \mathbf{F}_L - S_L \mathbf{F}_R + S_L S_R (\mathbf{U}_R - \mathbf{U}_L)}{S_R - S_L} & \text{if } S_L \leq 0 \leq S_R, \\ \mathbf{F}_R & \text{if } S_R \leq 0. \end{cases}$$

The wave speeds S_L and S_R must be estimated in some way, and one possibility is to use

$$S_L = u_L - a_L q_L, \quad S_R = u_R + a_R q_R.$$

3.1.2 Roe solver

Consider the non-linear Riemann problem in (2.4.1):

$$\mathbf{U}_t + \mathbf{F}(\mathbf{U})_x \equiv \mathbf{U}_t + \mathbf{A}\mathbf{U}_x = 0,$$

where \mathbf{A} is the Jacobian matrix of \mathbf{F} . The Roe solver is based on an approximation of the Jacobian matrix \mathbf{A} by a Roe matrix $\tilde{\mathbf{A}}$, which is a constant coefficient matrix, to obtain the linear system

$$\mathbf{U}_t + \tilde{\mathbf{A}}\mathbf{U}_x = 0.$$

This means that the Roe solver solves the approximated Riemann problem

$$\mathbf{U}_t + \tilde{\mathbf{A}}\mathbf{U}_x = 0.$$

$$\mathbb{U}(x, 0) = \begin{cases} \mathbf{U}_L, & x < 0, \\ \mathbf{U}_R, & x > 0. \end{cases}$$

exact. That is, the original non-linear conservation laws are replaced by a linearised system with constant coefficients.

The main idea in the Roe solver is to find average values $\tilde{h}, \tilde{a}, \tilde{u}$ and $\tilde{\psi}$ for the depth h , the celerity a (??), the velocity component u and the scalar ψ . The method thus use the following Roe averages:

$$\begin{cases} \tilde{h} = \sqrt{h_L h_R}, \\ \tilde{u} = \frac{u_L \sqrt{h_L} + u_R \sqrt{h_R}}{\sqrt{h_L} + \sqrt{h_R}}, \\ \tilde{a} = \sqrt{\frac{1}{2}(a_L^2 + a_R^2)}, \\ \tilde{\psi} = \frac{\psi_L \sqrt{h_L} + \psi_R \sqrt{h_R}}{\sqrt{h_L} + \sqrt{h_R}}. \end{cases} \quad (3.1.1)$$

The average eigenvalues (of what?) are

$$\tilde{\lambda}_1 = \tilde{u} - \tilde{a}, \quad \tilde{\lambda}_2 = \tilde{u}, \quad \tilde{\lambda}_3 = \tilde{u} + \tilde{a},$$

with the corresponding right eigenvectors

$$\tilde{\mathbf{R}}^{(1)} = \begin{bmatrix} 1 \\ \tilde{u} - \tilde{a} \\ \tilde{\psi} \end{bmatrix}, \quad \tilde{\mathbf{R}}^{(2)} = \begin{bmatrix} 0 \\ 0 \\ 1 \end{bmatrix}, \quad \tilde{\mathbf{R}}^{(3)} = \begin{bmatrix} 1 \\ \tilde{u} + \tilde{a} \\ \tilde{\psi} \end{bmatrix}.$$

The wave strenghts $\tilde{\alpha}_j$ described by Roe averages are given by

$$\begin{cases} \tilde{\alpha}_1 = \frac{1}{2} \left[\Delta h - \frac{\tilde{h}}{\tilde{a}} \Delta u \right], \\ \tilde{\alpha}_2 = \frac{1}{2} \left[\tilde{h} \Delta \psi \right], \\ \tilde{\alpha}_3 = \frac{1}{2} \left[\Delta h + \frac{\tilde{h}}{\tilde{a}} \Delta u \right]. \end{cases} \quad (3.1.2)$$

Applying theory of linear systems with constant coefficients. The numerical flux is

$$\mathbf{F}_{i+\frac{1}{2}} = \frac{1}{2} (\mathbf{F}_L + \mathbf{F}_R) - \frac{1}{2} \sum_{j=1}^3 \tilde{\alpha}_j \left| \tilde{\lambda}_j \right| \tilde{\mathbf{R}}^{(j)}. \quad (3.1.3)$$

The Roe flux (3.1.3) is used in the explicit conservative scheme to solve the SWE in 1D.

Entropy fix?

3.2 Implementation of the FVM in 1D

The code to solve the SWE in 1D using FVM is based on the Godunov scheme with the exact Riemann solver. The exact solution of the Riemann problem is found by using the Riemann invariants and the Rankine-Hugoniot conditions [7].

The true solution is found by solving the Riemann problem exact, with 5000 cells, and distinguishing between the wetbed or drybed case, and also identifying the shock and rarefaction waves.

3.3 Godunov's Method

We consider the Godunov Upwind method, which is a first-order accurate method to solve non-linear systems of hyperbolic conservation laws [4]. Godunov's method is a fundamental starting point. In the method we solve the non-linear Riemann problem at each cell interface.

Consider the initial-boundary value problem (IBVP) for a system of N nonlinear hyperbolic conservation (balance?) laws

$$\begin{cases} \text{PDEs:} & \mathbf{U}_t + \mathbf{F}(\mathbf{U})_x = \mathbf{S}(\mathbf{U}), \quad x \in [a, b], \quad t > 0, \\ \text{ICs:} & \mathbf{U}(x, 0) = \mathbf{U}^{(0)}(x), \quad x \in [a, b], \\ \text{BCs:} & \mathbf{U}(a, t) = \mathbf{B}_L(t), \quad \mathbf{U}(b, t) = \mathbf{B}_R(t), \quad t \geq 0. \end{cases} \quad (3.3.1)$$

The vectors $\mathbf{B}_L(t)$ and $\mathbf{B}_R(t)$ denote the boundary conditions at the left and right boundaries, respectively. The Godunov Upwind method in conservative form (2.3.1) solves the IBVP (3.3.1).

3.4 Data generation

The data generation is done by solving the SWE in 1D using the FVM with the Godunov scheme and the exact Riemann solver. We use Gaussian functions with parametric extension [8] to generate the initial conditions, that is, functions on the form

$$h(x, 0) = a \exp\left(\frac{-(x - \mu)^2}{2\sigma^2}\right),$$

where a is the amplitude of the Gaussian, μ is the mean value, and σ is the standard deviation. We solve the 1D SWE with the following parameters:

- $N = 200$ cells,
- From $t = 0.0$ to $t_{\text{end}} = 1.0$,
- $x \in [0, 1]$,
- $u(x, 0) = 0$,
- $b(x) = 0.0$,
- $g = 9.81$ and
- $\sigma = 0.1$.

The value of μ is varied to generate different initial conditions, as seen in Figure 3.1.

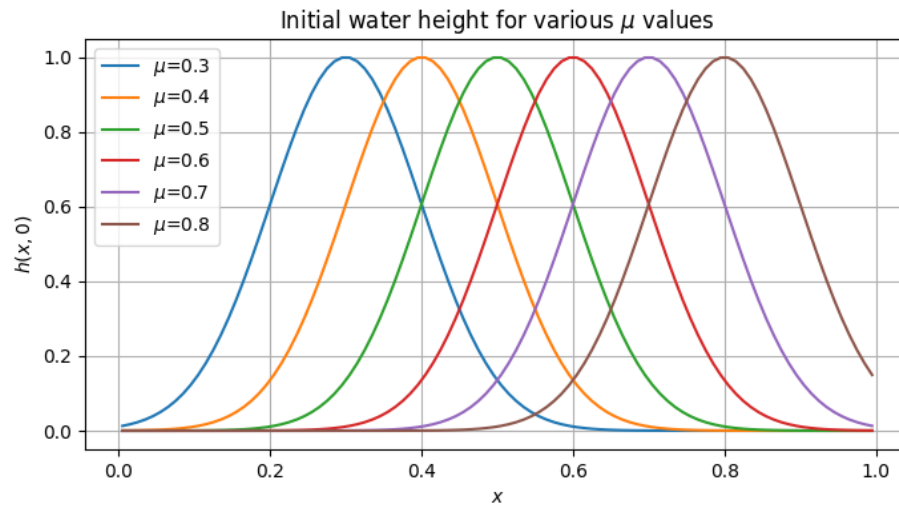


Figure 3.1: Initial conditions for the data generation.

Chapter 4

Numerical results

In this chapter we present the results of the numerical experiments, where we have implemented the Finite Volume Method for solving the shallow water equations in 1D and tested it on several problems.¹ A key focus is to verify the implementation, as it will be used to generate data for the data-driven methods, including neural networks and Fourier neural operators.

4.1 The 1D Dam Break Problem

First we solve the 1D dam break problem, which is a model of a dam suddenly breaking and the water flowing out. We consider a problem with the following initial conditions:

$$h(x, 0) = \begin{cases} h_L, & \text{if } x < x_0, \\ h_R, & \text{if } x > x_0, \end{cases}$$

where $x \in [0, 50]$, $h_L = 3.5m$, $h_R = 1.0m$ and $x_0 = 20m$. Since it is a dam break problem the initial fluid velocity is zero, i.e., $u(x, 0) = 0$. We solve the problem starting at $t = 0$ and ending at $t = 2.5$ seconds. The numerical solution to the 1D Dam Break Problem using the FVM, together with the true solution, provided from the course [9], can be seen in Figure 4.1.

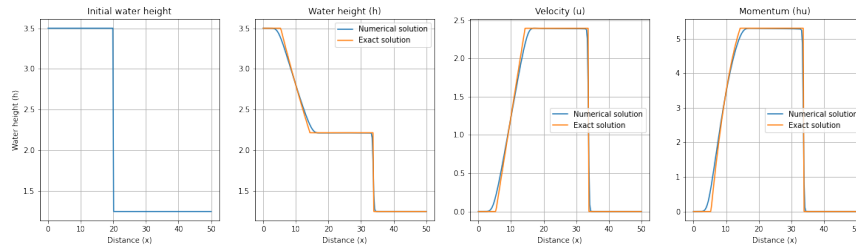


Figure 4.1: The initial water height h at $t = 0$, together with the water height, the fluid velocity u and the momentum hu after $t = 2.5$ seconds.

From Figure 4.1 we see that the numerical solution aligns well with the true solution, and successfully captures the discontinuity.

¹Code and small animations can be found at github, visit <https://github.com/MelissaJessen/Shallow-Water-Equations>.

4.2 Toro test cases

We have tested the method on the five test cases from Toros book [1]. The initial conditions for the five test cases are given in Table 4.1.

Test case	h_L	u_L	h_R	u_R	x_0	t_{end}
1	1.0	2.5	0.1	0.0	10.0	7.0
2	1.0	-5.0	1.0	5.0	25.0	2.5
3	1.0	0.0	0.0	0.0	20.0	4.0
4	0.0	0.0	1.0	0.0	30.0	4.0
5	0.1	-3.0	0.1	3.0	25.0	5.0

Table 4.1: Initial conditions for the five test cases.

The domain is $x \in [0, 50]$ for all test cases. The test cases are chosen to test the method on different types of waves, such as shock waves and rarefaction waves.

Test case 1

The initial conditions for test case 1 are given in Figure 4.2, and the final solution after $t = 7.0$ seconds is given in Figure 4.3. In test case 1, we observe a right shock wave and a left critical rarefaction wave.

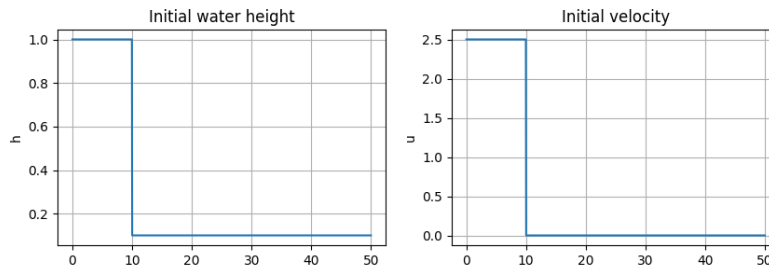


Figure 4.2: Initial conditions for the test case.

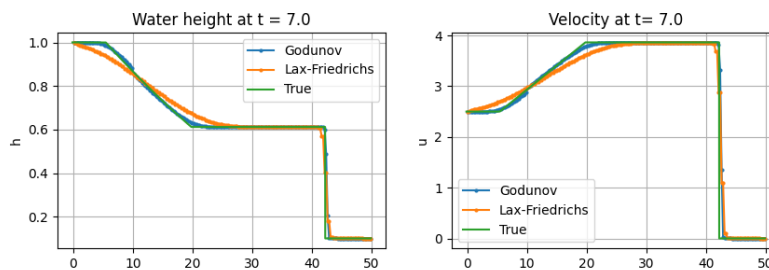


Figure 4.3: Final solution for the test case.

Test case 2

The initial conditions for test case 2 are illustrated in Figure 4.4.

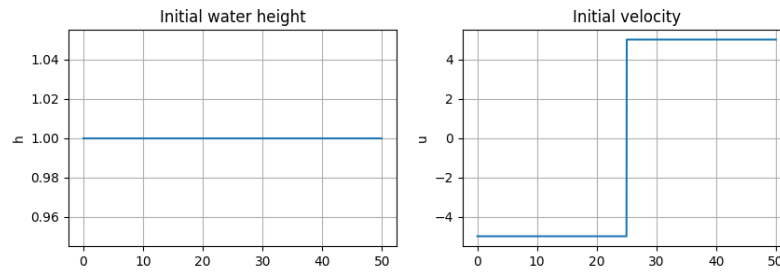


Figure 4.4: Initial conditions for the test case.

In test case 2 we have two rarefaction waves, one on the left side and one on the right side. As they are travelling in opposite directions (away from each other), there will be created a nearly dry bed in the middle of the domain. Many methods have difficulties with this test case as they may compute a negative water height. For these experiments we were able to get close to the true solution, using Lax-Friedrich flux, FORCE flux and HLLC flux. The final solution after $t = 2.5$ seconds is given in Figure 4.5.

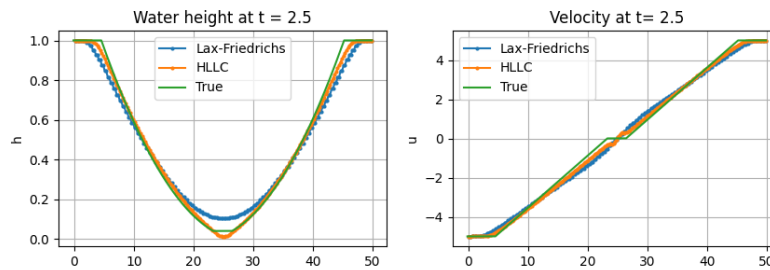


Figure 4.5: Final solution for the test case.

For some of the other fluxes, Godunov method with exact Riemann solver, Lax-Wendroff or flux-splitting/upwind, it was not possible to get an acceptable solution.

Test case 3

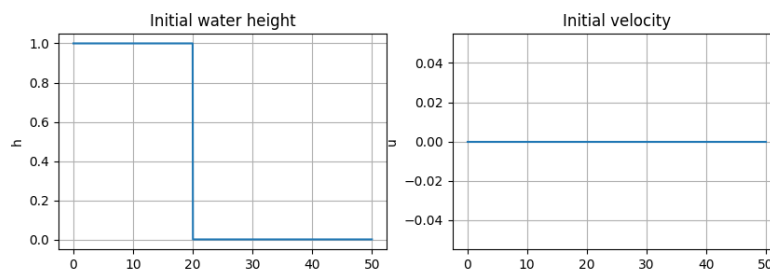


Figure 4.6: Initial conditions for the test case.

The problem is a left dry-bed problem.

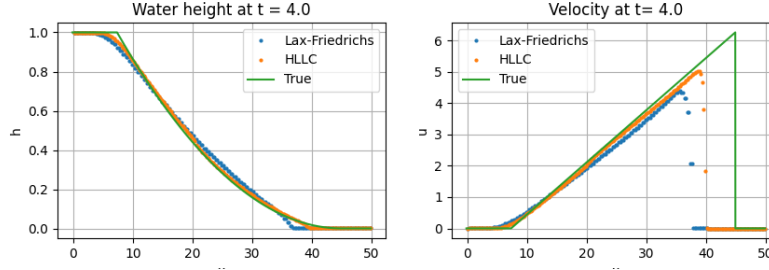


Figure 4.7: Final solution for the test case.

To solve case 3, with the FVM we must add a small amount to h_R , since the code does not handle $h_R = 0$ well. We set $h_R = 0.00005$. The true solution is for $h_R = 0$. By running experiments with different values of h_R , we see that the solution converges to the true solution as h_R approaches 0. The solution consists of a left rarefaction wave.

Test case 4

Test case 4:

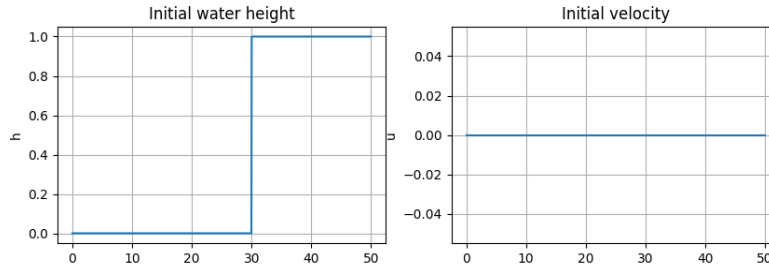


Figure 4.8: Initial conditions for the test case.

The problem is a right dry-bed problem.

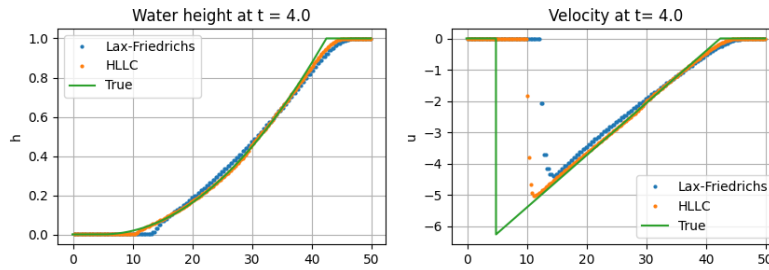


Figure 4.9: Final solution for the test case.

In case 4 we face the same challenges as in case 3. We set $h_L = 0.00005$, and the solution converges to the true solution as h_L approaches 0. This test case is symmetric to test case 3, and the solution consists of a right rarefaction wave. The case is included to test if the results are as expected.

Test case 5

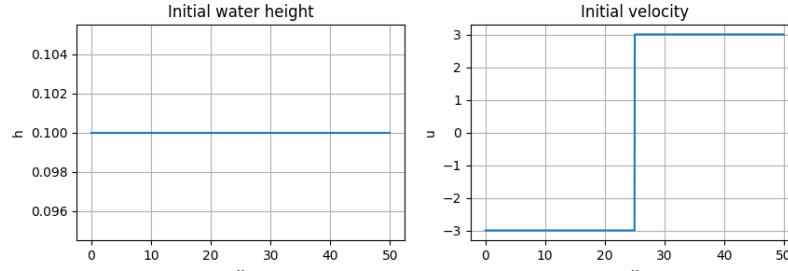


Figure 4.10: Initial conditions for the test case.

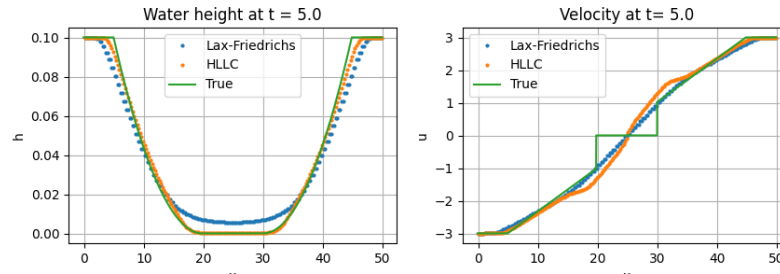


Figure 4.11: Final solution for the test case.

From Figure 4.11 we see that the numerical solutions for the velocity v at $t = 5.0$ are smooth, where the true solution is discontinuous. In this test case there are also challenges with some of the fluxes due to the generation of a dry-bed region. The fluxes that don't work are: Godunov method with exact RP, Lax-Wendroff and flux-splitting/upwind. The solution consists of two rarefaction waves, one on the left side and one on the right side, and a dry-bed region in the middle.

4.3 2D idealised Circular Dam Break Problem

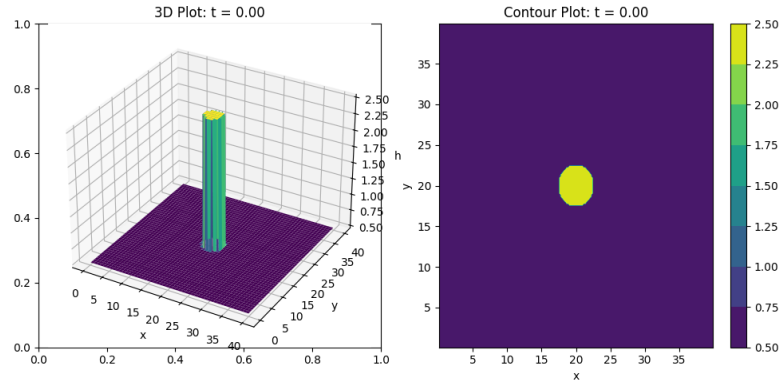
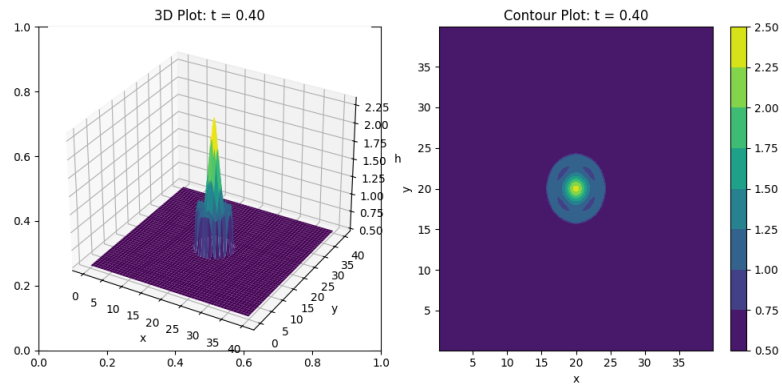
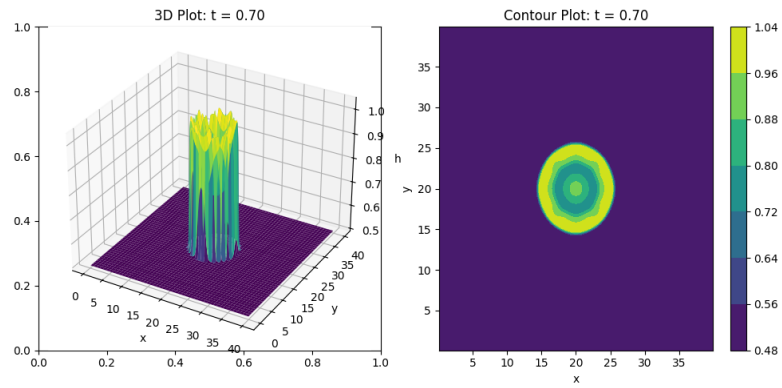
Consider the idealised circular dam break problem with a horizontal bottom. We assume there is an infinitely thin circular wall at radius $R = 2.5m$ in a square domain of size $40m \times 40m$ with centre at $(x_c, y_c) = (20m, 20m)$. The initial conditions are (ch. 15 Toro)

$$h(x, y, 0) = \begin{cases} 2.5 \text{ m}, & \text{if } \sqrt{(x - x_c)^2 + (y - y_c)^2} \leq R, \\ 0.5 \text{ m}, & \text{otherwise,} \end{cases}$$

$$u(x, y, 0) = 0,$$

$$v(x, y, 0) = 0.$$

Use the WAF method (chapter 11) along with a second-order dimensional splitting scheme (chapter 12). CFL-condition: $C_{cfl} = 0.9$. van Leer limiter. Mesh: 200×200 .

Figure 4.12: 2D dam break problem after $t = 0$.Figure 4.13: 2D dam break problem after $t = 0.4$.Figure 4.14: 2D dam break problem after $t = 0.7$.

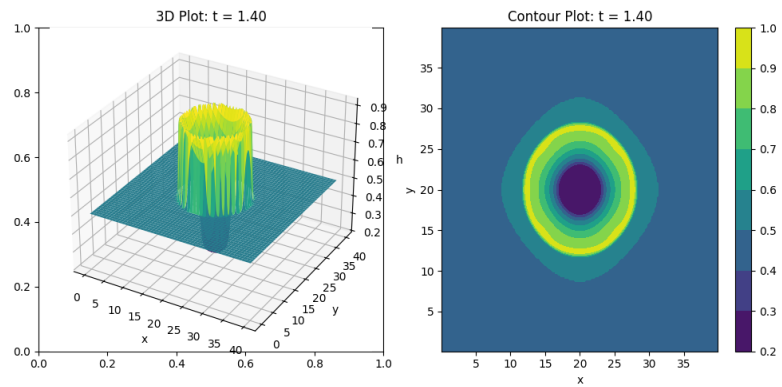


Figure 4.15: 2D dam break problem after $t = 1.4$.

Chapter 5

Discussion

In this project, we have implemented a Finite Volume Method to solve the shallow water equations in 1D, succesfully simulating the dam break problem.

Chapter 6

Further work

In this project, we have implemented a Finite Volume Method to solve the shallow water equations in 1D, successfully simulating the dam break problem. Although we attempted to extend this method to 2D, time constraints prevented us from completing it. We also began adapting the 1D method to accommodate a curved bottom surface instead of a flat one but couldn't finish this implementation either. Both extensions are promising, and it would be interesting to observe how the model performs with a curved bottom. Another interesting extension is to implement the FVM in 3D and use it to solve the SWE in spherical coordinates.

Bibliography

- [1] E.F. Toro. *Shock-Capturing Methods for Free-Surface Shallow Flows*. Oxford University Press, 2001.
- [2] C.B. Vreugdenhil. *Numerical Methods for Shallow-Water Flow*. Kluwer Academic Publishers, 1994.
- [3] Wikipedia. Leibniz integral rule. https://en.wikipedia.org/wiki/Leibniz_integral_rule, 7/10-2024.
- [4] E.F. Toro. *Computational Algorithms for Shallow Water Equations*. Springer, 2024.
- [5] Randall J. LeVeque. *Finite Volume Methods for Hyperbolic Problems*. Cambridge Texts in Applied Mathematics. Cambridge University Press, 2002.
- [6] E.F. Toro. *Riemann Solvers and Numerical Methods for Fluid Dynamics*. Springer, 2009.
- [7] Ilya Peshkov. Advanced numerical methods for environmental modeling. <https://www.unitn.it/dricam/1116/advanced-numerical-methods-environmental-modeling>, 2023. Lecture notes.
- [8] Wikipedia. Gaussian function. https://en.wikipedia.org/wiki/Gaussian_function, 14/10-2024.
- [9] A. P Engsig-Karup and J. S. Hesthaven. An introduction to discontinuous galerkin methods for solving partial differential equations. <https://www2.compute.dtu.dk/~apek/DGFEMCourse2009/>, 2009. Lecture notes.